

Covalently Linked Heterobimetallic Catalysts for Olefin Polymerization

Jiaxi Wang, Hongbo Li, Neng Guo, Liting Li, Charlotte L. Stern, and Tobin J. Marks*

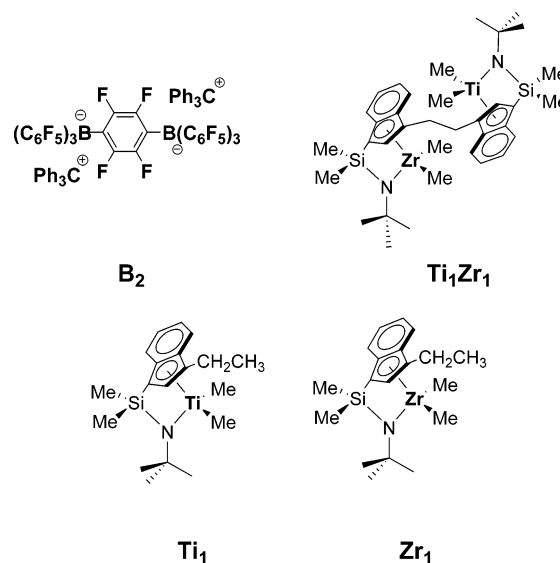
Department of Chemistry, Northwestern University, Evanston, Illinois 60208-3113

Received July 11, 2004

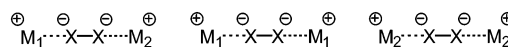
Summary: This contribution describes the synthesis and polymerization characteristics of the covalently linked heterobinuclear constrained-geometry polymerization catalyst $(\mu\text{-CH}_2\text{CH}_2\text{-3,3'})\{(\eta^5\text{-indenyl})[1\text{-Me}_2\text{Si}(\text{tBuN})](\text{TiMe}_2)\}\{(\eta^5\text{-indenyl})[1\text{-Me}_2\text{Si}(\text{tBuN})](\text{ZrMe}_2)\}$ (**Ti₁Zr₁**). When activated with $\text{Ph}_3\text{C}^+\text{B}(\text{C}_6\text{F}_5)^-\text{4}$, it is competent to produce long-chain ($\geq C_6$) branched polyethylenes in ethylene homopolymerization, in sharp contrast to control experiments with mixtures of analogous but mononuclear Zr and Ti CGC catalysts.

Linear low-density polyethylene (LLDPE)¹ is an important polymeric material that has attracted immense research interest due to its impressive rheological and mechanical properties—small but significant levels of C₄–C₆ alkyl branching lead to excellent processibility and high melt tensions suitable for film manufacture.² Typically, LLDPE branching is achieved via copolymerization of ethylene with a linear α -olefin comonomer. Single-site constrained-geometry catalysts (CGCs) represent another major advance in this field, since the polyethylene produced also contains long-chain branches arising from competing macromonomer re-enchainment.^{3,4} Homogeneous “tandem catalysis” has also received attention as an alternative approach to branched polyethylenes.^{5,6} Here, one single-site catalytic center produces α -olefin oligomers, which are subsequently incorporated into high-molecular-weight polyethylene by a second, different single-site catalytic center in the same reaction solution, utilizing the same ethylene

feed.⁶ Since this type of polymerization system requires intermolecular elimination + enchainment sequences at low catalyst concentrations, the attractive possibility of constraining two catalyst centers in close spatial proximity offers the potential for significantly enhanced efficiency. Previously, we demonstrated marked cooperative effects in *electrostatically joined* binuclear catalyst/cocatalyst combinations,^{7,8} where the binuclear activator/cocatalyst $[\text{Ph}_3\text{C}^+]_2[1,4\text{-(C}_6\text{F}_5)_3\text{BC}_6\text{F}_4\text{B(C}_6\text{F}_5)_3]^{2-}$ (**B₂**) can spatially confine pairs of cationic centers.⁸ However,



while electrostatic strategies can accentuate the unique characteristics of component heteronuclear pairs (M_1, M_2 ; by manipulating relative concentrations), they cannot exclusively select for them over other coexisting statistical components ($M_1, M_1 + M_2, M_2$) and greatly restrict the spectrum of applicable cocatalysts.



(6) (a) Komon, Z. J. A.; Diamond, G. M.; Leclerc, M. K.; Murphy, V.; Okazaki, M.; Bazan, G. C. *J. Am. Chem. Soc.* **2002**, *124*, 15280–15285. (b) Quijada, R.; Rojas, R.; Bazan, G. C.; Komon, Z. J. A.; Mauler, R. S.; Galland, G. B. *Macromolecules* **2001**, *34*, 2411–2417. (c) Komon, Z. J. A.; Bu, X.-H.; Bazan, G. C. *J. Am. Chem. Soc.* **2000**, *122*, 1830–1831. (d) Komon, Z. J. A.; Bu, X.-H.; Bazan, G. C. *J. Am. Chem. Soc.* **2000**, *122*, 12379–12380.

(7) For covalently linked homobinuclear systems, see: (a) Li, H.; Li, L.; Marks, T. J. *Angew. Chem., Int. Ed.*, in press. (b) Guo, N.; Li, L.; Marks, T. J. *J. Am. Chem. Soc.* **2004**, *126*, 6542–6543. (c) Li, H.; Li, L.; Marks, T. J.; Liable-Sands, L.; Rheingold, A. L. *J. Am. Chem. Soc.* **2003**, *125*, 10788–10789. (d) Li, L.; Metz, M. V.; Li, H.; Chen, M.-C.; Marks, T. J.; Liable-Sands, L.; Rheingold, A. L. *J. Am. Chem. Soc.* **2002**, *124*, 12725–12741.

(1) James, D. E. In *Encyclopedia of Polymer Science and Engineering*; Mark, H. F., Bikales, N. M., Overberger, C. G., Menges, G., Eds.; Wiley-Interscience: New York, 1985; Vol. 6, pp 429–454.

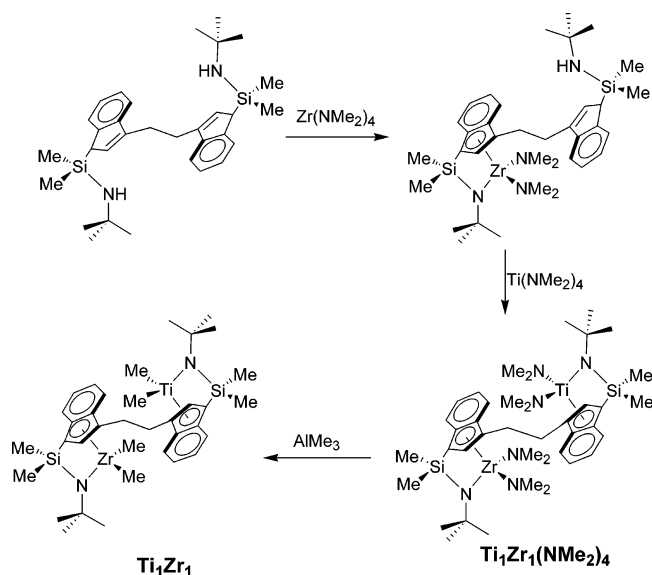
(2) (a) Jin, H.-J.; Kim, S.; Yoon, J.-S. *J. Appl. Polym. Sci.* **2002**, *84*, 1566–1571. (b) Starck, P.; Malmberg, A.; Lofgren, B. *J. Appl. Polym. Sci.* **2002**, *83*, 1140–1156. (c) Kulshrestha, A. K.; Talapatra, S. In *Handbook of Polyolefins*; Vasile, C., Ed.; Marcel Dekker: New York, 2000; pp 1–70. (d) Quijada, R.; Narvaez, A.; Rojas, R.; Rabagliati, F. M.; Galland, G. B.; Maules, R. S.; Benabente, R.; Perez, E.; Perena, J.; Bello, A. *Macromol. Chem. Phys.* **1999**, *200*, 1306. (e) Galland, G. B.; Seferin, M.; Mauler, R. S.; Dos S., Joao H. Z. *Polym. Int.* **1999**, *48*, 660–664. (f) Quijada, R.; Scipioni, R.; Mauler, R.; Galland, G.; Miranda, M. S. *Polym. Bull.* **1995**, *35*, 299. (g) Quijada, R.; Dupont, J.; Lacerda, M.; Scipione, R.; Galland, G. *Macromol. Chem. Phys.* **1995**, *196*, 3991.

(3) For recent reviews of single-site olefin polymerization, see: (a) Gibson, V. C.; Spitzmesser, S. K. *Chem. Rev.* **2003**, *103*, 283–316. (b) Gladysz, J. A.; Ed. *Chem. Rev.* **2000**, *100* (special issue on “Frontiers in Metal-Catalyzed Polymerization”). (c) *Top. Catal.* **1999**, *15*, and references therein (Marks, T. J., Stevens, J. C., Eds.).

(4) For constrained-geometry catalysts, see: (a) Iedema, P. D.; Hoefsloot, H. C. J. *Macromolecules* **2003**, *36*, 6632–6644. (b) Klosin, J.; Kruper, W. J., Jr.; Nickias, P. N.; Roof, G. R.; De Waele, P.; Abboud, K. A. *Organometallics* **2001**, *20*, 2663–2665. (c) McKnight, A. L.; Waymouth, R. M. *Chem. Rev.* **1998**, *98*, 2587–2598. (d) Lai, S. Y.; Wilson, J. R.; Knight, G. W.; Stevens, J. C. WO-93/08221, 1993.

(5) (a) Chen, E.-Y.; Marks, T. J. *Chem. Rev.* **2000**, *100*, 1391–1434. (b) Alt, H. G.; Köppl, A. *Chem. Rev.* **2000**, *100*, 1205–1221. (c) Britovsek, G. J. P.; Gibson, V. C.; Wass, D. F. *Angew. Chem., Int. Ed.* **1999**, *38*, 428–447. (d) Chen, E.-Y.; Metz, M. V.; Li, L.; Stern, C. L.; Marks, T. J. *J. Am. Chem. Soc.* **1998**, *120*, 6287–6305.

Scheme 1. Synthesis of the Heterobinuclear Catalyst Ti_1Zr_1



In an effort to fully exploit the potential of heteronuclear intramolecular cooperative effects, a new heterobinuclear complex, Ti_1Zr_1 , which covalently links Zr and Ti CGC moieties, has been designed. Here a monometallic Ti center should produce high- M_w polyethylenes with high activity,^{4c,d} while a mononuclear Zr center should produce low- M_w polyethylenes having reactive vinylic end groups with moderate activity.^{7d} In this contribution, we report the synthesis and characterization of Ti_1Zr_1 and preliminary ethylene polymerization results which reveal the catalyst is competent to produce long-chain ($\geq C_6$) branched polyethylenes in ethylene homopolymerization.

The heterobimetallic catalyst Ti_1Zr_1 was synthesized via the protodeamination, Al_2Me_6 alkylation methodology outlined in Scheme 1.⁹ The first step is the synthesis of the heterobimetallic amido complex $\text{Ti}_1\text{Zr}_1(\text{NMe}_2)_4$, via reaction of the free ($\mu\text{-CH}_2\text{CH}_2\text{-3,3'}$)[1-($\text{Me}_2\text{SiNH}^t\text{Bu}$)indeny]l₂ (EBICGCH₂) ligand with 1.0 equiv of Zr-(NMe_2)₄. The intermediate product is then subjected to reaction with 1.0 equiv of Ti(NMe_2)₄ to obtain $\text{Ti}_1\text{Zr}_1(\text{NMe}_2)_4$. The sequence of first adding Zr(NMe_2)₄ and then Ti(NMe_2)₄ is employed because the former undergoes protodeamination more rapidly and in a more selective, stepwise fashion. Furthermore, small amounts of the binuclear Zr₂ byproduct can be readily separated by filtration. Reaction of $\text{Ti}_1\text{Zr}_1(\text{NMe}_2)_4$ with excess AlMe_3 cleanly affords the dimethyl complex Ti_1Zr_1 . Both heterobinuclear complexes were characterized by a full complement of spectroscopic and analytical methodologies.⁹

The solid-state structure of $\text{Ti}_1\text{Zr}_1(\text{NMe}_2)_4$ was characterized by X-ray diffraction and is shown in Figure 1, which reveals that the Ti and Zr atoms are positionally disordered. The derived metal–ligand metrical parameters are essentially the average of those determined for similar homobinuclear Ti and Zr CGC complexes,^{7c,d,9} while the internal ligand distances and angles are unexceptional. That the product is indeed a hetero-

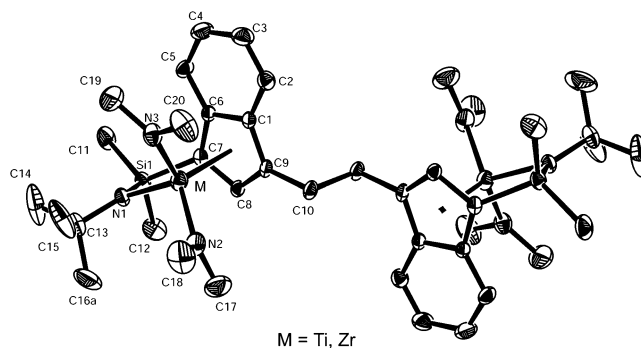


Figure 1. Crystal structure of $\text{Ti}_1\text{Zr}_1(\text{NMe}_2)_4$. Selected bond distances (Å) and angles (deg): M–N(1), 2.0684(8); M–N(2), 1.998(2); M–N(3), 1.991(2); M–C(1), 2.632(2); M–C(6), 2.558(2); M–C(7), 2.442(2); M–C(8), 2.482(2); M–C(9), 2.559(2); N(3)–M–N(2), 105.05(9); N(3)–M–N(1), 107.14(8); N(2)–M–N(1), 106.30(8); N(1)–Si(1)–C(7), 95.31(9). Thermal ellipsoids are drawn at the 50% probability level. Note that the Ti and Zr atoms are statistically disordered.

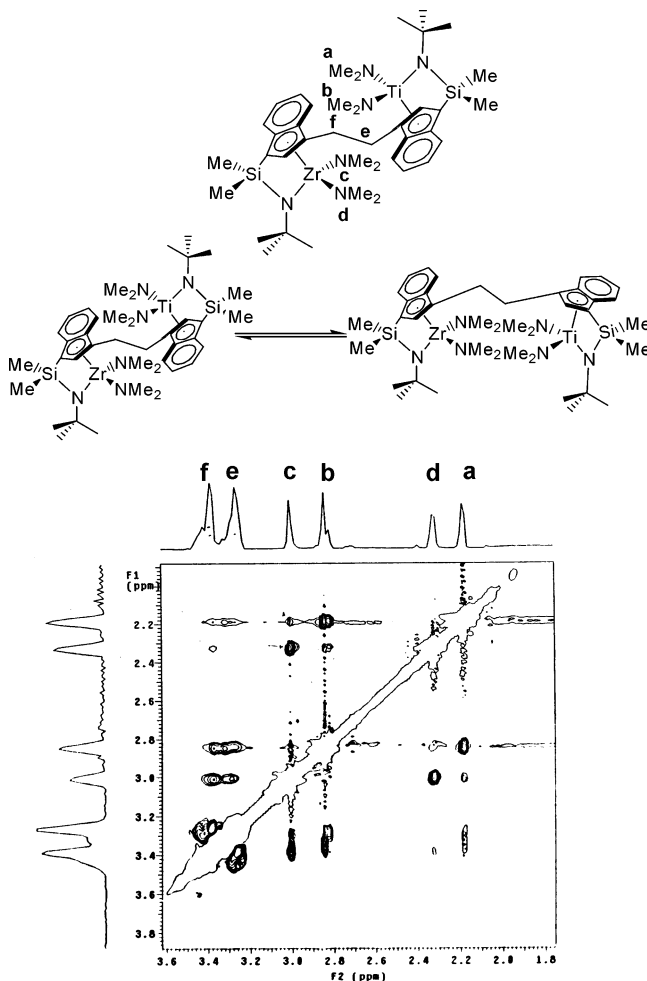


Figure 2. 2D NOESY ^1H NMR spectrum of $\text{Ti}_1\text{Zr}_1(\text{NMe}_2)_4$.

nuclear complex is further supported by 2D ^1H NMR NOESY spectroscopy,⁹ which reveals in conjunction with the assignments for the homobinuclear analogues^{7c,d} that the methyl signals from the Zr– NMe_2 and Ti– NMe_2 moieties have cross-peaks, indicating that the Zr and Ti moieties are present within the same molecule (Figure 2). Ti_1Zr_1 was also characterized by 1D ^1H and ^{13}C NMR spectroscopy and elemental analysis. The ESI

(8) Abramo, G. P.; Li, L.; Marks, T. J. *J Am. Chem. Soc.* **2002**, *124*(47), 13966–13967.

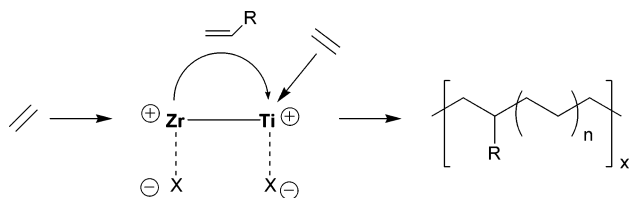
(9) Details of the Ti_1Zr_1 synthesis, analysis, and polymerization experiments are provided in the Supporting Information.

Table 1. Ethylene Polymerization Results for Ti_1Zr_1 Catalysts^a

entry	catalyst	conditions ^b	polymer yield (g)	activity ^c	M_w ^d	M_w/M_n ^d	LCB ($\geq C_6$)/1000C ^e
1	Ti_1Zr_1	24, 5	0.43	5.2×10^5	779 000	2.09	~0
2	Ti_1Zr_1	44, 3	0.55	1.1×10^6	929 000	1.39	1.0
3	Ti_1Zr_1	64, 1	0.46	2.8×10^6	782 000	1.64	2.1
4 ^f	Zr_1	24, 15	0.35	1.4×10^5	730	1.10	0.7
5	Zr_1	64, 4	0.95	1.4×10^6	690	1.20	0.8
6	Ti_1	24, 1	1.67	1.0×10^7	171 000	2.31	~0
7	Ti_1	64, 1	2.52	1.5×10^7	121 000	1.64	~0
8	$\text{Ti}_1 + \text{Zr}_1$ (1:1)	64, 1	0.46	2.8×10^6	238 000, 650	2.54, 1.30	~0

^a Polymerizations were carried out in 100 mL of toluene under 1.0 atm of ethylene; the catalyst loading was 10 μmol , with trityl tetrakis(pentafluorophenyl)borate as cocatalyst. ^b Conditions given: temperature of polymerization in $^\circ\text{C}$, reaction time in min. ^c In units of g of polymer/[mol of metal] atm h]. ^d From GPC with universal calibration using polystyrene standards. ^e Long chain branches ($\geq C_6$) calculated from ^{13}C NMR (error range of ± 0.2 C/1000 C). ^f From ref 7d.

Scheme 2. Possible Scenario for Enhanced Polyolefin Chain Branching Mediated by a Covalently Joined Heterobinuclear Catalyst



mass spectrum⁹ of Ti_1Zr_1 reveals a prominent fragment corresponding to $\text{C}_{26}\text{H}_{28}\text{N}_2\text{Si}_2\text{TiZr}$ (m/z 563.3, with a consistent isotopic pattern), likely reflecting the loss of *tert*-butyl groups; no homobinuclear fragments can be detected.

Olefin polymerization experiments were carried out under rigorously anhydrous/anaerobic conditions with attention to exotherm and mass transfer effects.^{7–9} From the ethylene polymerization results (Table 1), it can be seen that the catalyst $\text{Ti}_1\text{Zr}_1 + 2\text{Ph}_3\text{C}^+\text{B}(\text{C}_6\text{F}_5)_4^-$ produces high-molecular-weight polyethylene with high activity. The monomodal GPC traces and product polydispersities are consistent with single-site processes (entries 1–3), while the greater polyolefin molecular weights produced by the binuclear catalyst appear to reflect a type of cooperative effect on propagation vs chain transfer rates observed previously.^{7a} Moreover, the ^{13}C NMR data indicate that the Ti_1Zr_1 -derived polyethylenes have as many as an average of 2.1 long-chain ($\geq C_6$) branches/1000 carbon atoms. In contrast to these results, a 1:1 mixture of mononuclear $\text{Me}_2\text{Si}(\text{BuN})(\eta^5\text{-3-ethylindenyl})\text{ZrMe}_2$ (Zr_1)^{7d} and $\text{Me}_2\text{Si}(\text{BuN})(\eta^5\text{-3-ethylindenyl})\text{TiMe}_2$ (Ti_1)^{7c} + $\text{Ph}_3\text{C}^+\text{B}(\text{C}_6\text{F}_5)_4^-$ as catalysts (entry 8) generates polymeric products with a bimodal polydispersity and negligible branching. This result argues that the covalently linking heterobimetallic sites in Ti_1Zr_1 spatially confine the Zr and Ti catalytic sites in such a way as to significantly increase the efficiency of intramolecular oligomer/macromonomer capture/enchainment, as suggested in Scheme 2. Note from entries 1–3 that the branching level in the polymer structures increases with increasing polymerization temperature. These results are consistent with the calculated relative chain transfer rates of the individual Zr and Ti catalyst moieties as a function of temperature. Specifically, it can be seen in control experiments with the mononuclear catalyst Zr_1 (Table 1, entry 5 vs entry 4) that polymerization activity increases $\sim 10\times$ from 24 to 64 $^\circ\text{C}$, while Ti_1 activity increases only $\sim 1.5\times$ over the same temperature range (entry 7 vs entry 6). Assuming for the moment that such activity ratios can

be directly transferred to the behavior of Ti_1Zr_1 , then at higher temperatures, the greater relative Zr/Ti polymerization activity will provide greater quantities of Zr-derived oligomers ($\sim 6.7\times$, with approximately the same M_w) for branch formation for a given polymer yield.

For single-site polymerization, M_n is typically proportional to the net rate of chain propagation divided by the net rate of chain termination, and if the net rate of chain propagation is proportional to the polymerization activity (reasonably assuming comparable percentages of active catalytic centers),^{7a} then the relative termination rate of mononuclear Zr_1 vs Ti_1 can be calculated from the M_n values and activities of these two catalysts. At 24 $^\circ\text{C}$, the calculated relative termination rate of mononuclear Zr_1 vs Ti_1 is 1.6, and the maximum branching level (assuming the majority of Zr-derived oligomers are efficiently captured by the Ti moiety) estimated for Ti_1Zr_1 is 1.6 branches per polyethylene chain (0.06 branches/1000 C), which is far below the ^{13}C NMR detection limit, consistent with the experimental results. At 64 $^\circ\text{C}$, the calculated polyethylene branching level introduced by Ti_1Zr_1 is predicted on the basis of the mononuclear catalyst results to be ~ 0.4 branches/1000C. As can be seen in Table 1, entry 3, the branching content is even greater than predicted by this admittedly crude estimate and likely reflects the interplay of metal–metal cooperative and ion-pair effects on the relative rates of propagation, chain transfer, and comonomer enchainment. Studies with other cocatalysts and comonomers are in progress to better understand these effects.

In summary, we report here for the first time the synthesis of the covalently linked, heterobinuclear, constrained-geometry polymerization catalyst, Ti_1Zr_1 . It produces long-chain branched polyethylene in ethylene homopolymerization, in sharp contrast to control experiments involving Zr and Ti tandem catalyst mixtures. The branch formation pathway is proposed to involve intramolecular cooperative effects.

Acknowledgment. This research was supported by the NSF (Grant No. CHE0415407) and the DOE (Grant No. 86ER13511). L.L. thanks Dow Chemical for a postdoctoral fellowship. We thank Dr. C. Zuccaccia for assistance with the NOE experiments.

Supporting Information Available: Text and figures giving details of Ti_1Zr_1 synthesis, characterization, and polymerization experiments and a CIF files giving X-ray crystallographic data. This material is available free of charge via the Internet at <http://pubs.acs.org>.

OM049481B